Influence of bed slope and friction on the linear stability of planar beaches

M.D. Klein[(1)] and H.M. Schuttelaars[(1,2)]

(1) Delft University of Technology, Faculty of Civil Engineering, Stevinweg 1, P.O.Box 5048, 2600 GA Delft, The Netherlands, m.d.klein@ct.tudelft.nl
(2) Institute for Marine and Atmospheric Science, Utrecht University, Princetonplein 5, 3584 CC Utrecht, The Netherlands, h.m.schuttelaars@phys.uu.nl

Abstract
A fully non-linear numerical model has been used to perform a linear stability analysis on planar sloping beaches. One of the main advantages of using a fully nonlinear model is the fact that no simplifications with respect to the physical formulation has to be made. This paper focuses on the influence of friction and bed slope on the wavelength, growth and migration rates of the fastest growing mode. The bed perturbation that has been found in all but one case is an up-current bar with two maxima. From the stability analysis it is found that an increase in the drag coefficient yields a decreasing wavelength and an increasing growth rate. Increasing the bed slope results in smaller wavelengths, whereas the growth rate has a maximum for a bed slope of 1%, irrespective of the friction coefficient. Furthermore, multiple modes, with different bed perturbations, exist in case of high friction and a small bed slope.

1. Introduction
Rhythmic coastal features have often been observed on both planar and barred beaches and have been the subject of many studies as well. Rhythmic features like oblique bars, rip channel systems and beach cusps exist on length scales varying from one to eight times the surfzone width. The time scale at which these features significantly change is much smaller (of the order of days) than the time scale at which the underlying cross-shore profile shows a significant change. Different theoretical explanations for the generation of these observed rhythmic patterns have been given in the literature. One explanation focuses on the effects of direct hydrodynamic forcing (see Holman and Bowen, 1982), whereas self-organization in the coupled hydro- and morphodynamic system has been proposed to clarify the observations as well. This last explanation can be studied by performing a linear stability analysis (LSA).
The first one to study the surf zone morphology with a stability model was Hino (1974). He found down-current oriented bars with a spacing of about four times the surfzone width x_b (the orientation of the bar is defined with respect to the point of shore attachment). Hino's study was extended by Christensen et al. (1994) by enhancing the formulation of the physical processes like wave forcing and sediment transport. Applying a sediment transport relation that depended linearly on the local velocity with a uniform wave stirring resulted in up-current oriented bars with a spacing of about six times the surf zone width. Ribas et al. (2003) further extended the previous studies by structurally exploring the influence of the angle of wave incidence, the parameterization of wave stirring and the formulation of the sediment transport. In case of a sediment transport relation that depended linearly on the local velocity, and stirring that was proportional to the squared wave height, representative of wave-dominated beaches, down-flow migrating, crescentic bar features were found. For angles of wave incidence larger than 5°, the inner bar was down-current oriented and the wavelength of the crestentic bars was about the width of the surf zone. For smaller angles the direction of migration altered, whereas the bed perturbation did not significantly change its shape.
In the LSA's mentioned above, many simplifications had to be made to be able to explicitly linearize the hydro- and morphodynamic equations, e.g. simplifications with repect to the wave forcing and linearized bottom shear stress. In the study presented here, the stability properties of the surf zone morphology are studied with a fully non-linear numerical model. No simplifications in the model formulations have to be made, a wide range of parameters can be investigated and any type of coast can be studied. The method to determine the most unstable bed perturbation and its growth- and migration rate in a fully non-linear

model has already been used by Deigaard et al. (1999) and Klein et al. (2002) and will be discussed in more detail in section 2.
Amonst the parameters studied in Ribas et al. (2003), the sensitivity of *r*, the ratio of the drag coefficient and the bed slope parameter, was studied. Increasing *r* had a damping effect on the results, i.e. smaller growth rates for larger *r*, but the alongshore spacing and the spatial structure of the bed perturbation were hardly influenced by *r*. However, the two parameters were not studied in separation. In this study the influence of the drag coefficient and the bed slope parameter on the fastest growing mode are studied in separation. Furthermore, since a state-of-the-art formulation of the bed shear stress is used, the influence of the parameterization used in Ribas et al (2003) can be assessed.
Section 2 describes the model formulations and the method used to determine the most unstable mode. Section 3 presents the results of this study, Section 4 discusses these results and the conclusions are finally drawn in Section 5.

2. Model formulations and method

Figure 1 presents the orientation of the coordinate system and the definitions of the bed slope *b*, wave height *H*, total water depth *D* and the position of the breaker line x_b.

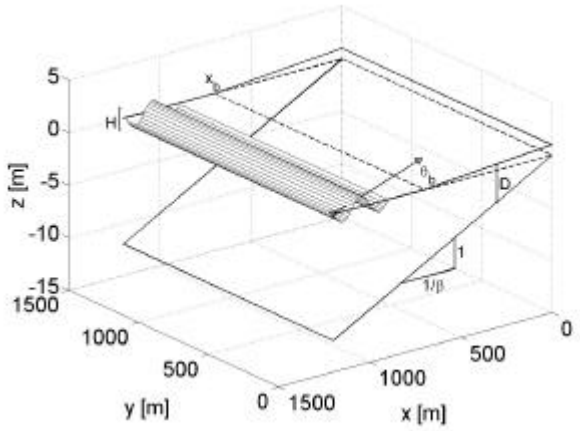

Figure 1. Definition sketch.

The cross-shore coordinate *x* is zero on the beach and positive in offshore direction and the alongshore coordinate is *y*. The cross-shore current velocity *u* is positive in offshore direction and the longshore current velocity *v* is positive in positive *y* direction. The still water level is at *z* = 0. The water motion is described by the non-linear, depth-averaged shallow water equations, consisting of the momentum equations and the mass conservation equation, Eqs. 1 and 2, respectively:

$$\frac{\partial \vec{u}}{\partial t} + \vec{u}\nabla\vec{u} + g\nabla z_s + \frac{\vec{t}}{r\,D} + \frac{\vec{F}}{r\,D} - n\nabla^2\vec{u} = 0 \qquad (1)$$

$$\frac{\partial z_s}{\partial t} + \nabla(D\vec{u}) = 0 \qquad (2)$$

In these equations, $\vec{u}$ is the current velocity vector, *t* the time, *g* the gravitational acceleration, z_s the water level, $\vec{t}$ the bed shear stress vector, *r* the water density, *D* the total water depth, $\vec{F}$ the wave force vector and *n* the turbulent eddy viscosity. The parameterization of Soulsby et al. (1993) for the bed shear stress due to waves and currents has been used. The eddy viscosity *n* has been set to one. Note that the water motion is only forced by gradients in the radiation stresses. The radiation stresses are computed with the second generation wave model HISWA, see Holthuijsen et al. (1989) using the formulation proposed by Dingemans et al. (1987). A consequence of this formulation is that the wave set-down in the shoaling zone is not computed, since that set-down is caused by wave height variations and not by dissipation. As flow

boundary conditions the longshore current velocities along the shore-perpendicular boundaries are prescribed. This has to be done in an iterative way such that the longshore current profile is consistent with the wave forcing under consideration. On the seaward, shore-parallel boundary a zero water level is prescribed.
The bed evolves due to convergence and divergence of sediment fluxes, which are computed with a simple sediment transport formula derived from Bailard's formulation (Bailard, 1981) of bed load transport in wave-dominated circumstances. This enables us to compare the results with Ribas et al. (2003) who considered this case as well (by putting $m = 1$ in their transport formulation). Hence, the sediment transport relation is the same and reads:

$$\vec{q} = a(x)|\vec{u}|\left(\frac{\vec{u}}{|\vec{u}|} - g\nabla h'\right) \tag{4}$$

This formulation accounts for stirring due to short waves and bed slope related transport. The wave stirring parameter $a(x)$ is assumed to be proportional to the squared wave height. Bed slope effects have been neglected in this study by setting g to zero. It has been verified that g has a damping effect and its influence on the shape of the bed perturbation is limited.
This system of equations allows for a morphological equilibrium solution $F = F_{eq}$, with $F = F(u,v,D)$, when the system is forced with waves, whose characteristics like angle of incidence and wave height do not vary in longshore direction. This equilibrium state is alongshore uniform, i.e. the bathymetry and the longshore current $v(x)$ only have a cross-shore structure, whereas the cross-shore velocity u is zero. It is not clear whether or not this morphological equilibrium is stable. Therefore a LSA is performed. The equilibrium bed profile is disturbed with a small bed perturbation, periodic in the alongshore direction:

$$h'(x,y) = \mathrm{Re}(A_i(x)\exp[iky - iwt]) \tag{5}$$

Here $h'(x,y)$ is the bed perturbation, $A_i(x)$ the complex cross-shore amplitude function, k the alongshore wave number, $?$ the complex angular frequency (eigenvalue) and i the imaginary unit. The alongshore wave number can be chosen freely, whereas the cross-shore amplitude function and the complex eigenvalue are solutions of the eigenvalue problem. The imaginary part ($?_i$) of the complex eigenvalue represents the growth rate of the perturbation and the real part ($?_r$) the alongshore migration of the perturbation.
Since the water motion is calculated with a fully non-linear, process-based model a formal linearization cannot be performed. In order to mimic the linear system, the amplitude of the perturbation should be chosen sufficiently small, such that non-linear terms are negligible in the equations. In practice this is realized by choosing a bed perturbation amplitude that is not larger than 1% of the local water depth in the complete computational domain.
An iteration process has to be used to find the solution with the largest positive real part of the eigenvalue, i.e. the solution that initially grows fastest. In order to start the iteration process, we need to make a first guess of the cross-shore amplitude function of the perturbation. It was verified that the final solution is independent of the initially chosen cross-shore amplitude distribution. During every iteration the cross-shore amplitude function A_i, which only contains the bed perturbation related to the wave number k, is derived using a Fourier analysis. This amplitude distribution is rescaled such that the amplitude is again smaller than 1% of the local water depth. Based on the previous cross-shore amplitude $A_{i-1}(x)$ of the perturbation and the newly computed one, $A_i(x)$, an estimate for the complex eigenvalue $?$ is obtained. This estimate is based on the Rayleigh quotient (Griffel, 1985):

$$R(A_{i-1}) = -iw = \frac{\int_{-\infty}^{0} A_{i-1}^{*}(x)A_i(x)dx}{\int_{-\infty}^{0} A_{i-1}^{*}(x)A_{i-1}(x)dx} \tag{6}$$

in which * denotes the complex conjugate. This Rayleigh quotient is an estimate of the eigenvalue with largest real part. The problem has been defined such that the real part of the Rayleigh quotient corresponds with the growth rate. By repeatedly determining the Rayleigh quotient in an iterative process, the eigenvalue can be exactly determined. By constructing a new perturbation for every iteration step, based on the results of the last iteration, the estimated eigenvalue will converge towards the exact eigenvalue. The accuracy criterion for convergence has been set to 0.5%, i.e. if both the real and imaginary part of the eigenvalue change less than 0.5%, the iteration process is assumed to have converged. In that case, $A_i(x)$ gives the cross-shore structure of the eigenfunction.
Note that this iteration process is only done for one wavelength. For that specific wavelength one mode is found, the one with the largest growth rate. Repeating this process for a range of the wavelengths, a maximum growth rate can be identified. The mode with this wavelength is the fastest growing mode (FGM). The stability analysis has mainly been performed for wavelengths that are a multiple of 100 m.
The model and the method that have been used limit the wavelengths that can be considered. The model domain measures $6\times1.2\ km^2$ divided in $10\times10\ m^2$ grid cells. The domain of analysis is at least 1 km or one wavelength away from the model boundary. In order to be able to consider wavelengths smaller than about 200 m, the model should consist of smaller grid cells than have been used now. The computational effort does not allow for such a change. On the other hand, wavelengths larger than about 1200 m (depending on the drag coefficient) cannot be considered in this model since disturbances from the model boundary enter the area in which the Fourier analysis necessary to determine the FGM is performed.

3. Results

In this section the results of the LSA are presented. All results are obtained with q_b = 10°, H_s = 1.1 m and g_b = 0.8. These wave conditions are representative for the yearly-averaged wave conditions along the Dutch coast. Furthermore, n = 1 m^2s^{-1}, $a(x)=0.01H(x)^2$, c_d = 0.0025 and b = 0.01. These values are the default values and have been used in the reference case. In the following, the influence of the friction coefficient is investigated. Values of the drag coefficient used are 0.0020, 0.0025 and 0.0035. These friction values range from a 'normal' value (0.0035) to a rather low value (0.0020). Furthermore, the influence of the bed slope on the results is presented. Bed slopes considered are 0.0075, 0.01 and 0.0125. These values for the slope are reasonable values for many coasts, such as the Dutch coast, although much steeper coast exist as well, like the Duck coast. An overview of the experiments that have been performed and the results regarding the growth rate w_i, migration celerity c and the wavelength l_p of the FGM of each set of experiments are summarized in Table 1. The migration celerity has been obtained by dividing the migration rate w_r by the wave number k.

Table 1. Performed experiments and their summarized results

		b			
		0.0075		0.01	0.0125
c_d	0.0035	$l_{p1} < 250\ m$ $w_i > 4.55e\text{-}6\ s^{-1}$ $c < 0.0008\ ms^{-1}$	$l_{p2} = 660\ m$ $w_i = 3.67e\text{-}6\ s^{-1}$ $c = 0.0010\ ms^{-1}$	$l_p = 650\ m$ $w_i = 3.99e\text{-}6\ s^{-1}$ $c = 0.0011\ ms^{-1}$	$l_p = 550\ m$ $w_i = 3.94e\text{-}6\ s^{-1}$ $c = 0.0011\ ms^{-1}$
	0.0025	$l_p = 800\ m$ $w_i = 2.60e\text{-}6\ s^{-1}$ $c = 0.0011\ ms^{-1}$		$l_p = 700\ m$ $w_i = 2.96e\text{-}6\ s^{-1}$ $c = 0.0012\ ms^{-1}$	$l_p = 600\ m$ $w_i = 2.91e\text{-}6\ s^{-1}$ $c = 0.0012\ ms^{-1}$
	0.0020	$l_p = 1000\ m$ $w_i = 2.05e\text{-}6\ s^{-1}$ $c = 0.0012\ ms^{-1}$		$l_p = 900\ m$ $w_i = 2.36e\text{-}6\ s^{-1}$ $c = 0.0013\ ms^{-1}$	$l_p = 800\ m$ $w_i = 2.18e\text{-}6\ s^{-1}$ $c = 0.013\ ms^{-1}$

3.1 Equilibrium state

Figure 2 presents the bed level z_b, water level h, the root-mean-square wave height H_{rms} and the longshore current velocity profile $v(x)$ corresponding to the equilibrium state. Besides, the Longuet-Higgins longshore current velocity profile corresponding to the applied forcing is plotted as well. In this

experiment, the default parameters were used. Since HISWA uses irregular waves, H_{rms} instead of H is plotted. Due to the irregularity of the waves, the longshore current velocity profile is smoother than the Longuet-Higgins profile.

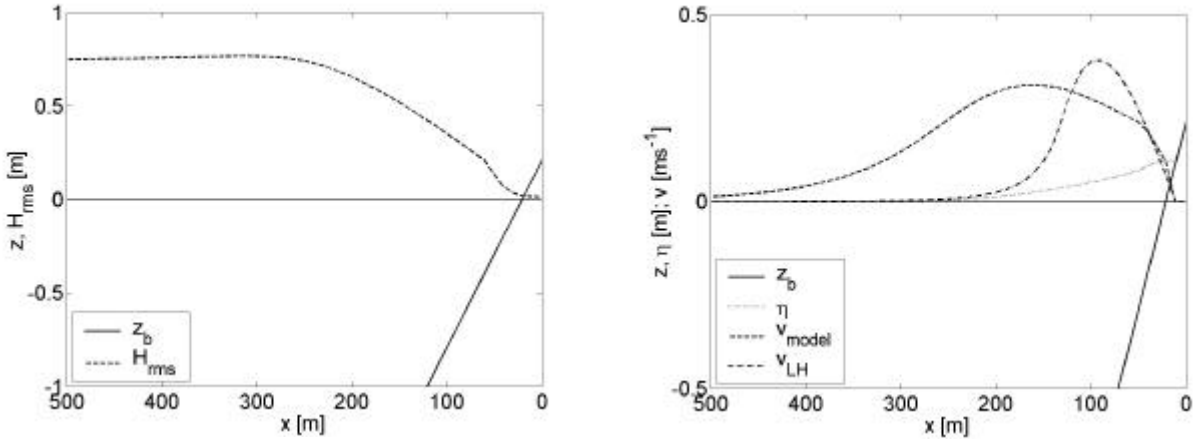

Figure 2. RMS wave height (left panel) and water level and longshore current velocity corresponding to the equilibrium state (right panel). The corresponding Longuet-Higgins profile is plotted as well.

3.2 Reference case

In this section the linear stability of a beach using the reference characteristic parameters is investigated. For a range of alongshore wavelengths the spatial structure and the corresponding growth rates and migration celerities have been determined. Figure 3 presents the growth rate w_i and the migration celerity c vs. the wavelength. One can clearly see that there is a maximum growth rate at l = 700 m. This mode is designated as the fastest growing mode (FGM). Also the migration celerity has a maximum value, although its maximum does not occur for the FGM but for a mode with a smaller wavelength.

The bed and flow perturbations of the FGM of this reference case are presented in Figure 4. It clearly shows that the bed perturbation is a crescentic feature, with an up-current oriented inner bar. The line of maximum wave energy dissipation has been drawn as well, as a measure for the surf zone width. It is clear that the bed perturbation shows a maximum both inside and outside the breaker zone. The wavelength of the FGM is about three times the surf zone width.

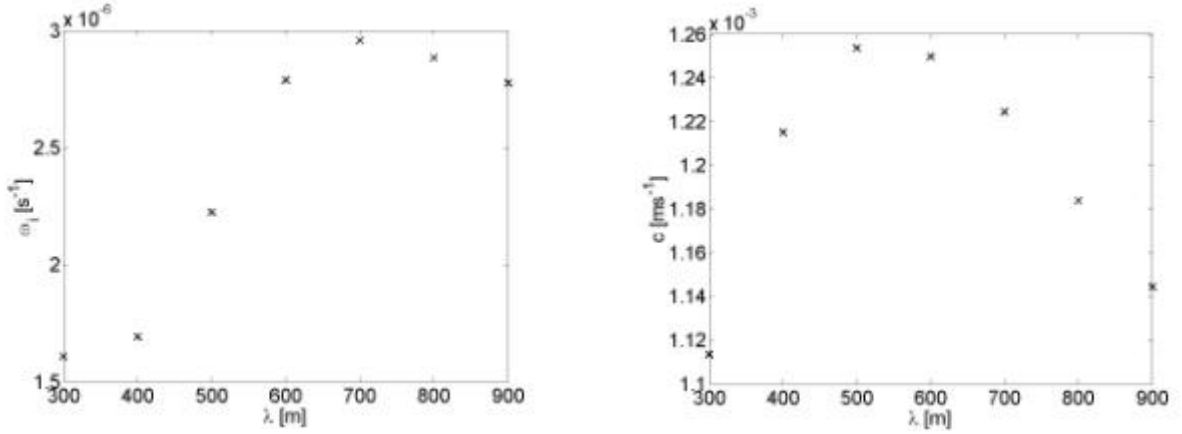

Figure 3. Growth rate vs. wavelength (left panel) and migration celerity vs. wavelength (right panel).

3.3 Influence of the drag coefficient

From Table 1 it is clear that an increase in the drag coefficient leads to a decrease in l_p, whereas the growth rate increases. The migration rate increases with decreasing friction. The bed shear stress hardly

has an influence on the spatial structure. The bed perturbations are very similar to the bed perturbation of the reference case, see Figure 4.

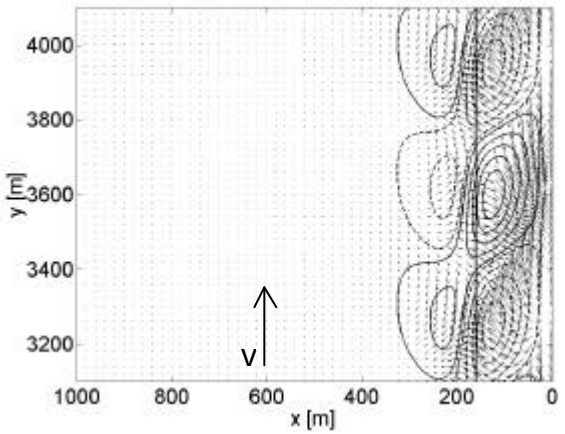

Figure 4. The bed and flow perturbation corresponding to the FGM of the reference case. Solid contours are shoals. The solid, straight line indicates the location of maximum wave energy dissipation.

3.4 Influence of the bed slope parameter

From Table 1 the influence of the bed slope parameter can be summarized as follows:

- The dependence of the growth rate on the bed slope is persistent for the three considered friction cases, viz. growth rates are largest for b = 0.01, and smaller for b = 0.0075 and 0.0125. Note that this is also true for b = 0.0075 and c_d = 0.0035, when considering the bed perturbation with l = 660 *m*. This will be discussed in more detail below.
- Although the influence of the bed slope on the migration celerity is rather limited, the migration celerity increases with increasing bed slope.
- The smaller the bed slope, the larger the wavelength. Despite variations in the breaker zone width due to variations in the bed slope, l_p is three to four times the surf zone width.

The bed slope parameter has, like the bed friction, hardly any influence on the shapes of the bed perturbation which are very similar to the one of the reference case, displayed in Figure 4.

In case of c_d = 0.0035 and b = 0.0075 two local maxima in the growth rate have been found for l = 570 and 660 *m*, see Figure 5. For wavelengths smaller than 500 *m* the growth rate increases with decreasing wavelength, without finding a maximum in the wavelength range considered. When looking at the bed perturbations (Figure 6) corresponding to l = 300 *m* and l = 660 *m*, one can see that the bed perturbations of these two cases differ. The larger wavelengths have two maxima, whereas the perturbations with smaller wavelengths only have one.

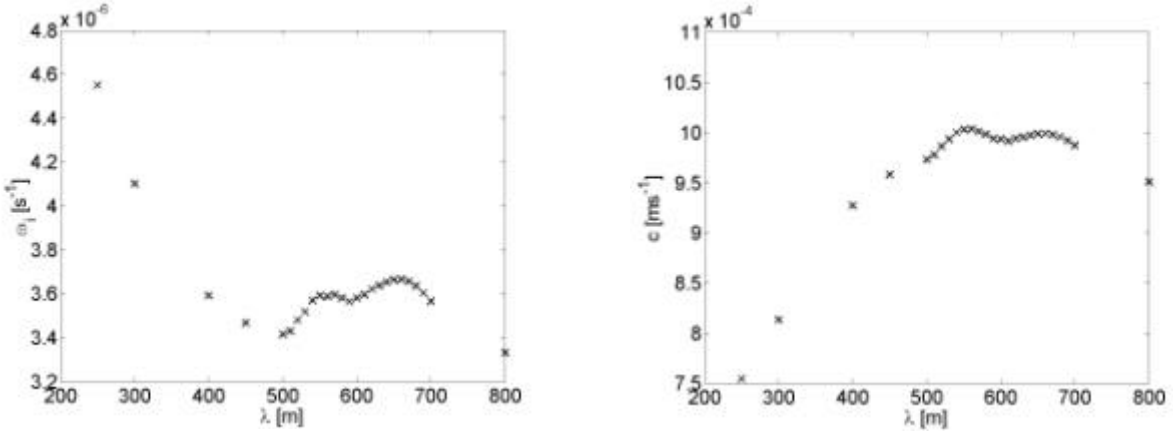

Figure 5. Growth rate vs. wavelength (left panel) and migration celerity vs. wavelength (right panel) in case of c_d = 0.0035 and b = 0.0075.

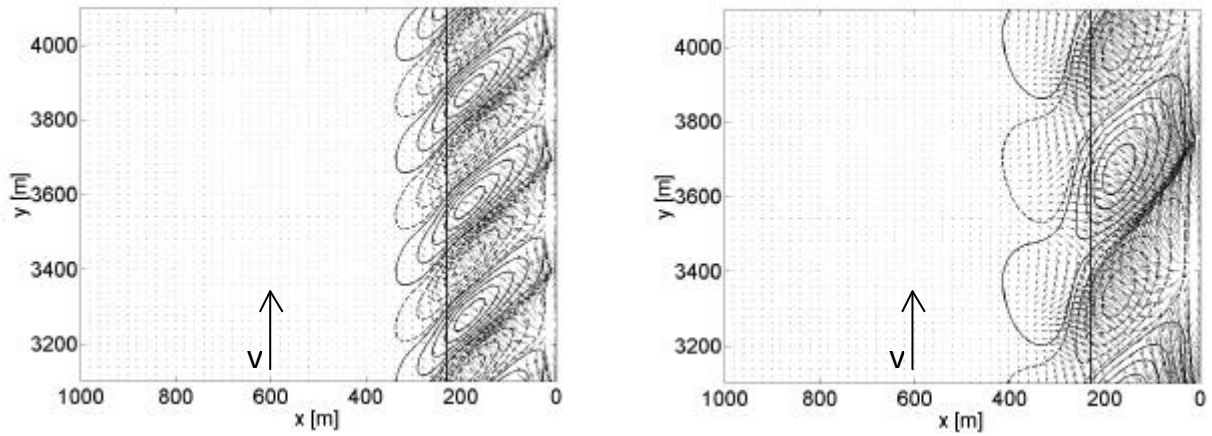

Figure 6. Bed perturbations in case c_d = 0.0035 and b = 0.0075 for l = 300 m (left panel) and λ = 660 m (right panel). The longshore current is directed in positive y direction.

These two different spatial structures are very similar to the spatial structures of the first and secondary mode (A1 and A2) found by Ribas et al. (2003), except for the orientation of the inner bar, which is up-current in the present study but down-current in Ribas et al. (2003). Also the perturbed velocity fields of the two wavelength cases differ, although the differences exist on a detailed level. Both observations suggest, however, that different modes have been found, also for l = 570 m. Due to the wavelength limitations of this model (i.e. the numerical constraints discussed at the end of section 2) this suggestion cannot be proved yet.

Discussion

In general we can state that the growth rates found in the present study are about four times smaller than the ones obtained by Christensen et al. (1994). They, however, used a different breaker wave height (3 m) and a different bed slope (0.04). In order to compare the absolute values of the growth rate with the ones obtained by Ribas et al. (2003) a scaling with a morphological time factor needs to done. This is left for further research.

In Ribas et al. (2003) the instability mechanism is described. In case of a linear sediment transport relation and a stirring that is proportional to the squared wave height, they showed that the growth of a shoal in the surf zone needs an onshore directed current, whereas the growth of a shoal outside the surfzone needs an offshore directed current. When looking at Figures 4 and 6, one can clearly see that the perturbed flow field corresponds with these theoretical considerations. Hence it can be concluded that the instability mechanism is reminiscent of the mechanism described in detail in Ribas et al. (2003).

In Ribas et al. (2003) it is suggested that the results only depend on the ratio of c_d and b. However, varying both c_d and b in such a way that their ratio does not change does not yield similar results: The FGM corresponding to c_d = 0.0020 and b = 0.01 differs considerably from the FGM corresponding to c_d = 0.0025 and b = 0.0125 regarding wavelength l_p as well as growth rate w_i and migration celerity c. However, at this moment the model formulation as used in Ribas et al. (2003) and the formulation used in this paper differ considerably (i.e. different formulation of the bed shear stresses and wave forcing). Therefore, the influence of the difference in formulation on the observed FGM will be investigated in more detail in the near future.

The effect of friction on the wavelength l_p is quite evident. The larger the friction, the smaller the current velocities, the smaller inertia effects are and thereby reducing, as suggested by both Deigaard et al. (1999) and Klein et al. (2002), the longshore spacing of the rhythmic pattern. The same holds for the migration celerity. The influence of friction on the growth rate, however, is less evident. Since the velocities are

higher for smaller friction, one would expect larger growth rates for smaller friction. We, however, find opposite results.
The bed slope does not only influence the current velocity directly by changing the relative importance of friction, but it also influences the wave forcing. Waves break in a more concentrated zone on a steep slope than on a mild slope. From the results it appears that the steeper the slope, the narrower the velocity profile and the higher the maximum velocity. Reasoning from inertia one would expect larger wavelengths for steeper slopes, but again the results show the opposite behaviour. Furthermore, the occurrence of a maximum in the growth rate for a bed slope of 1%, irrespective of the drag coefficient is remarkable. Two opposing mechanisms seem to be present causing this behaviour. These two mechanisms might also be responsible for the dependence of the growth growth rate on the drag coefficient and the dependence of the wavelength on the bed slope. These mechanisms, however, have not yet been identified.

Conclusions

The linear stability of planar sloping beaches has been studied with a state-of-the-art numerical model, with the focus on the influence of bed friction and bed slope. Up-current bars with a longshore spacing of three to four times surf zone width have been found in all but one case. In case of high friction and a mild slope, three modes have been found.
Increasing friction results in smaller wavelengths and smaller migration celerities. Both observations can be explained in terms of inertia. The growth rate increases with increasing friction. As to variations in the bed slope parameter, increasing the bed slope results in smaller wavelengths and in larger migration celerities. These smaller wavelengths cannot be explained from inertia considerations, whereas the migration rates can, since the maximum current velocity increases with increasing slope, yielding larger sediment transport rates that enable faster migration. The growth rates show a maximum for a bed slope of 1%. Both the influence of the friction parameter on the growth rate and the sensitivity for bed slope variations are currently under investigation.

References

J.A. Bailard, An energetics total load sediment transport model for a plane sloping beach, *J. Geophys. Res.* Vol. 86 (C11), pp. 10938-10954, 1981.
E.D. Christensen, R. Deigaard and J. Fredsøe, Sea bed stability on a long straight coast, *Proc. 24th Int. Conf. on Coast. Eng.*, pp. 1865-1879, 1994.
R. Deigaard, N. Drønen, J. Fredsøe, J.H. Jensen and M.P. Jørgensen, A morphological stability analysis for a long straight barred coast, *Coastal Engineering* 36, pp. 171-195, 1999.
M.W. Dingemans, A.C. Radder and H.J. de Vriend, Computations of driving forces of wave-induced currents, *Coastal Engineering* 11, pp. 539-563, 1989.
N. Dodd, On the destabilization of a longshore current on a plane beach: Bottom shear stress, critical conditions, and onset of instability, *J. Geophys. Res.* Vol. 99 (C1), pp. 811-824, 1994.
D.H. Griffel, *Applied functional analysis*, Ellis Horwood, New York, 1985.
M. Hino, Theory of formation of rip-current and cuspidal coast, *Proc. 14th Int. Conf. on Coast. Eng.*, pp. 901-919, 1974.
R.A. Holman and A.J. Bowen, Bars, bumps and holes: Models for the generation of complex beach topography, *J. Geophys. Res.* Vol. 87, pp. 457-468, 1982.
L.H. Holthuijsen, N. Booij and T.H.C. Herbers, A prediction model for stationary, short-crested waves in shallow water with ambient currents, *Coastal Engineering*, 13, pp. 23-54, 1989.
M.D. Klein, H.M. Schuttelaars and M.J.F. Stive, Linear stability of a double-barred beach, *Proc. 28th Int. Conf. on Coast. Eng.*, pp. 3396-3408, 2002.
M.S. Longuet-Higgins, Longshore currents generated by obliquely incident sea waves, 2, *J. Geophys. Res.* Vol. 75 (33), pp. 6790-6801, 1970.
F. Ribas, A. Falqués and A. Montoto, Nearshore oblique sand bars, *J. Geophys. Res.*Vol. 108 (C4), 3119, doi:10.1029/2001JC000985.
R.L. Soulsby, L. Hamm, G. Klopman, D. Myrhaug, R.R. Simons and G.P. Thomas, Wave-current interactions within and outside the bottom boundary layer, *Coastal Engineering* 21, pp. 41-69, 1993.